Journal of Physics: Conference Series **653** (2015) 012045 doi:10.1088/1742-6596/653/1/012045

Numerical investigations of shock wave propagation in polymethylmethacrylate

T V Popova[1], A E Mayer[1] and K V Khishchenko[2]

[1] Chelyabinsk State University, Bratiev Kashirinykh Street 129, Chelyabinsk 454001, Russia
[2] Joint Institute for High Temperatures of the Russian Academy of Sciences, Izhorskaya 13 Bldg 2, Moscow 125412, Russia

E-mail: tatyana_maskaeva@mail.ru

Abstract. Using the Maxwell model of viscoelastic medium, we numerically investigate the influence of the viscoelastic properties of polymethylmethacrylate on the variation of the shock wave amplitude with depth. Parameters of the Maxwell model are chosen by comparison with experimental data on the high-speed impact of plates in order to fit the modeling results with the experimentally measured profiles of the free-surface velocity. A caloric equation of state is used to calculate the pressure from density and internal energy. It is shown that at the limit of weak shock waves, the accounting of the viscoelastic properties allows one to achieve a better agreement between calculated and experimental data for the magnitude of the shock wave velocity in comparison with the case of hydrodynamic calculations. Using the viscoelastic and hydrodynamic approaches, we investigated the dynamics of shock waves in polymethylmethacrylate initiated by micro-, nano- and picosecond pulses of pressure on the sample surface. The calculation results show that the changes in the shock wave amplitude with depth are approximately identical in the hydrodynamic and viscoelastic cases.

1. Introduction

Characteristics of numerous substances, especially metals, are carefully studied in high-velocity tests [1–5]. High-molecular compounds, which represent a valuable class of substances, are less studied [6–8]. These include polymeric materials such as polymethylmethacrylate (PMMA, Plexiglas). The interest in studying the process of damage in polymers, in particular PMMA, is due to the fact that this material has unique physical properties and is widely used in various structures working in laser environments.

Many physical phenomena associated with the dynamic deformation of polymeric materials are accompanied by the formation and interaction of shock waves [9]. The impact of flyer plates driven to known velocities creates well-controlled conditions of loading. A number of experimental studies address deformation and damage of PMMA at quasistatic and dynamic loading [10–16]. An important phenomenon of shock-wave dynamics in the loaded material is the effect of spallation [17].

To determine the spall strength of materials, some authors [14–16] use the approach based on measuring the depth of the resulting hole, left by the spalled piece after the intensive pulsed laser action on the target, and the velocity of the spalled layer with subsequent mathematical modeling of the shock-wave process within the studied target [18]. This approach is sensitive to the correctness of shock dynamics calculations.

Here, we numerically investigate the influence of the viscoelastic properties of PMMA on the shock-wave dynamics. The dynamics of matter is modeled in the framework of the Maxwell model in comparison with the hydrodynamic approximation. The shock wave is initiated by micro-, nano- and picosecond pulses of pressure on the surface of PMMA. Such pulses model the effects of intense radiation of different time ranges.

2. Mathematical model

The high-speed impact or irradiation of PMMA plates can be treated as a one-dimensional problem as the plate thickness is much smaller than its lateral size or the beam diameter; the material deformation is uniaxial in this case. The basic system of continuum mechanics equations [19] is the following:

$$\frac{d\rho}{dt} = -\rho\frac{\partial \upsilon}{\partial z}, \tag{1}$$

$$\frac{d\upsilon}{dt} = \rho^{-1}\frac{\partial \sigma}{\partial z}, \tag{2}$$

$$\rho\frac{dE}{dt} = \sigma\frac{\partial \upsilon}{\partial z}, \tag{3}$$

where υ is the substance velocity; ρ is the density; $\sigma = -P + S_{zz}$ is the combined stress; P is the pressure; S_{zz} is the stress deviator; E is the internal energy. The system consists of the equation of continuity (1), the equation of motion (2) and the equation of internal energy (3). The system should be supplemented with an equation for the stress deviator (Hooke law) [20]

$$S_{zz} = 2G\left[\frac{2}{3}u_{zz} - w_{zz}\right], \tag{4}$$

where G is the shear modulus; w_{zz} is the component of the plastic strain tensor; u_{zz} is the component of the macroscopic strain tensor, which is defined by the macroscopic motion of matter:

$$\frac{du_{zz}}{dt} = \frac{\partial \upsilon}{\partial z}, \tag{5}$$

We refer the velocity, pressure and density to certain particles of the continuous medium moving in space in the course of time.

Behavior of polymeric materials can be classified as a viscoelastic one [21–23]. We use the Maxwell model for considering this property. At the series connection, tension in each element is the same, while the general deformation consists of deformation of the elastic element and deformation of the viscous one. In this case we can write [20]:

$$\frac{dS_{zz}}{dt} = G\left(\frac{4}{3}\frac{du_{zz}}{dt} - \frac{S_{zz}}{\eta}\right), \tag{6}$$

where η is the viscosity coefficient. Substituting the stress deviator (4) in Eq. (6) we can find the equation of plastic deformation:

$$\frac{dw_{zz}}{dt} = \left(\frac{2}{3}u_{zz} - w_{zz}\right)\tau^{-1}, \tag{7}$$

where $\tau = \eta/G$ is the relaxation time. The plastic flow in polymers starts, when the value of the stress deviator S_{zz} exceeds the threshold y_b characterizing the static yield stress; generalization of Eq. (7) is the following:

$$\frac{dw_{zz}}{dt} = \left(\frac{2}{3}u_{zz} - w_{zz} - \frac{y_b}{2G}\right)\tau^{-1} \times \theta\left(|S_{zz}| - y_b\right), \tag{8}$$

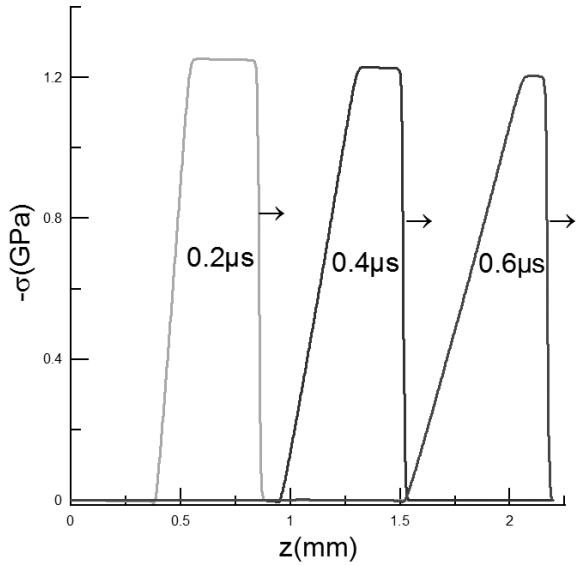

Figure 1. Shock propagation in PMMA.

where θ is the Heaviside function.

The caloric equation of state [24,25] is used to calculate the dependence of pressure on specific volume $V = 1/\rho$ and internal energy E.

The numerical solution of the continuum mechanics equations (1)–(3) is performed using the numerical method proposed by Yalovets [26].

Equations (4) and (8) are solved by the explicit Euler method.

3. Comparison of the simulation results with the experimental data

A standard test of material properties is a flat high-velocity impact of an impactor plate on a target plate [27]: the impactor hits the sample initiating a shock wave. A release wave arises in the impactor after shock circulation, which then propagates into the sample behind the shock wave. Characteristic profiles of the shock wave followed by the release wave at successive times are shown in figure 1; the impactor and target material is PMMA; the impactor thickness is 0.2 mm; the impactor velocity is 645 m/s.

In the experiments [11], the shock wave propagates through a sample of 6.35 mm thickness; the rear surface of the sample is attached to the window. The thickness of the impactor is also 6.35 mm. The material of both impactor and target is PMMA. The experiments [11] included continuous measurements of the velocity of the samples rear surface $u_{fs}(t)$ for various impactor velocities. Appearance of the shock wave front leads to the increase in the rear surface velocity. Appearance of the unloading wave on the samples rear surface causes a decrease in its velocity.

Results of the comparison of numerical modeling by the Maxwell model with the experimental data [11] are presented in figure 2. The calculations were done on a numerical grid of 600 cells. The wave profile is characterized by an initially sharp growth (during the time about nanoseconds) of the material velocity to about two-thirds of the maximum value. This is followed by a smooth increase in the material velocity to the peak value, and then the velocity remains constant for some time up to the arrival of the release wave. A close fit of the calculated and experimental data for the shock wave front is observed in figure 2; as for the release wave, the correspondence is considerably worse. The results presented in figure 2 are calculated with the following parameters of the Maxwell model: $G = 1.5$ GPa [28], $\tau = 0.4$ μs, $y_b = 38$ MPa.

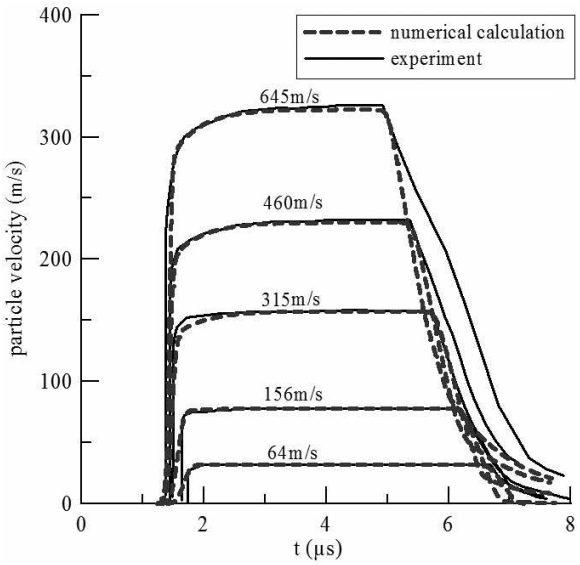

Figure 2. Velocity profiles of the rear surface of the PMMA samples. Calculations by the Maxwell model.

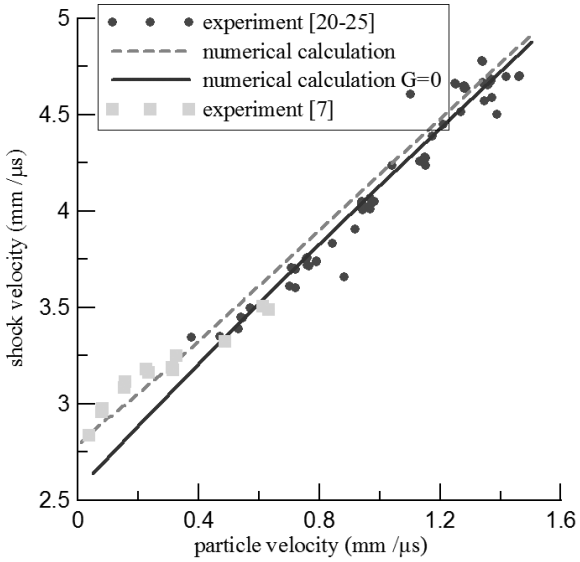

Figure 3. Dependence of the shock wave velocity on the particle velocity jump: numerical simulations in the hydrodynamic and viscoelastic approximations in comparison with the experimental data [11, 29–34].

These parameters correspond to the best coincidence with the experimental data. The results of our calculations qualitatively correspond to the results of modeling in [21, 22] also done by the Maxwell model.

Figure 3 shows the dependence of the shock wave velocity on the material velocity jump: the results of numerical modeling are compared with the experimental data [11, 29–34]. The calculations are performed in the viscoelastic approximation (Maxwell model) and in the hydrodynamic approximation. For intensive shock waves, the results for both models differ

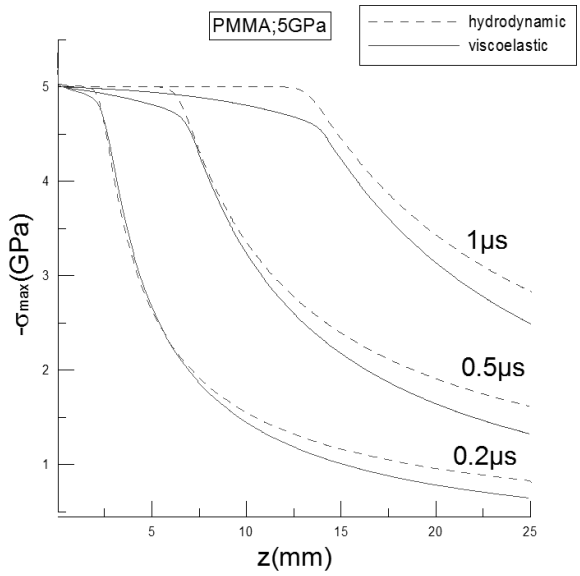

Figure 4. Spatial distributions of the maximum values of combined stresses in PMMA. The pressure amplitude is 5 GPa; the pulse durations are 0.2, 0.5 and 1 μs. Calculations in hydrodynamic (dashed line) and viscoelastic (continuous line) approximations.

insignificantly and correspond to the experimental data. The accounting of viscoelastic properties allows one to achieve a better coincidence with the experimental data in the range of low particle velocities. As the shock wave intensity tends to zero, the shock wave velocity tends to the value larger than the bulk sound velocity.

4. Shock wave overtaking by the release wave

Figures 4–6 show the plots of the shock wave amplitude as a function of depth, which reflect attenuation of the shock wave due to the overtaking by the release wave in the process of propagation deep into the target. The shock waves are initiated by micro-, nano- and picosecond pressure pulses on the PMMA surface. After the pressure pulse ceases, a release wave arises and propagates behind the shock wave. The figures show the results of both hydrodynamic (dashed line) and viscoelastic (continuous line) calculations. At first, the shock wave amplitude remains constant until the release wave reaches the shock wave front. Then, the interaction of the shock and release waves leads to a fast decrease in the shock wave amplitude, which is observed in figures 4–6.

The dependence of the maximum combined stress on coordinate for the microsecond pressure pulses are presented in figure 4. The graphs show that the release wave reaches the shock wave at a depth from 5 to 15 mm. The calculated curves for the hydrodynamic and viscoelastic cases are practically identical. The plots for the nanosecond pressure pulses are presented in figure 5; the release wave reaches the shock wave at a depth from 0.1 to 0.8 mm. In the viscoelastic case, the shock attenuation is slower than in the hydrodynamic approximation, but the difference decreases with increase in pressure. Figure 6 shows the results for the picosecond pressure pulses. The graphs show that the release wave reaches the shock wave at a depth from 0.0001 to 0.005 mm. In the viscoelastic case, the attenuation is slower than in the hydrodynamic approximation. In the whole, figures 4–6 show that the shock wave dynamics is not very different in the viscoelastic and hydrodynamic cases in the investigated range of pulse durations.

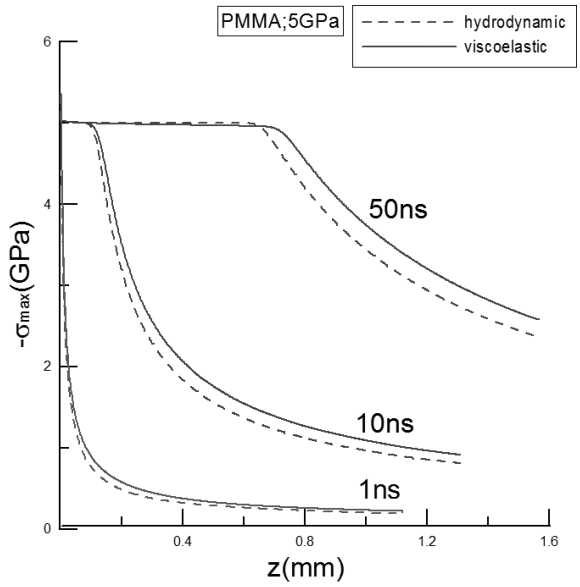

Figure 5. Spatial distributions of the maximum values of combined stresses in PMMA. The pressure amplitude is 5 GPa; the pulse durations are 1, 10 and 50 ns. Calculations in hydrodynamic (dashed line) and viscoelastic (continuous line) approximations.

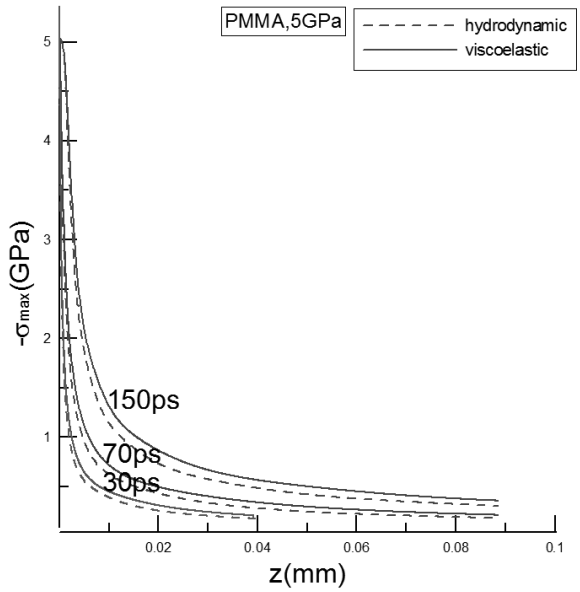

Figure 6. Spatial distributions of the maximum values of combined stresses in PMMA. The pressure amplitude is 5 GPa; the pulse durations are 30, 70 and 150 ps. Calculations in hydrodynamic (dashed line) and viscoelastic (continuous line) approximations.

5. Conclusion

Using the Maxwell model of viscoelastic matter, we numerically investigate the influence of viscoelastic properties of polymethylmethacrylate on the change in the shock wave amplitude with depth. Parameters of the Maxwell model are chosen by comparison with experimental data

on the high-speed impact of plates in order to fit the modeling results with the experimentally measured profiles of the free-surface velocity. A caloric equation of state is used to calculate the pressure from density and internal energy.

The Maxwell model with constant relaxation time allows us to describe the structure of the shock wave front; the release wave is described much less accurately. The results of comparison of the numerical calculations with the experimental data are presented. Profiles of the free-surface velocity and dependence of the shock wave velocity on the particle velocity jump are calculated. Taking into account the viscoelastic properties of the material provides a better description of the dependence of the shock-wave velocity on the particle velocity jump at low impact velocities. According to [13], viscoelastic properties also play an important role at laser-induced damage of PMMA. The calculated results show that the shock wave dynamics is not very different in the viscoelastic and hydrodynamic cases in the investigated range of pulse durations.

Acknowledgments

The authors appreciate sincerely Tatiana Zezyulina for English improvement of the paper. This work is supported by the Ministry of Education and Science of the Russian Federation (state task No. 3.1334.2014/K) and by grants from the President of the Russian Federation (No. MD-286.2014.1 and NSh-6614.2014.2) and the Russian Foundation for Basic Research (No. 14-08-00967).

References

[1] Kanel G I, Garkushin G V, Savinykh A S, Razorenov S V, de Resseguier T, Proud W G and Tyutin M R 2014 *J. Appl. Phys.* **116** 143504
[2] Kanel G I, Razorenov S V, Garkushin G V, Ashitkov S I, Komarov P S and Agranat M B 2014 *Phys. Solid State* **56** 1569–1573
[3] Razorenov S V, Garkushin G V, Kanel G I and Popov N N 2009 *J. Appl. Phys.* **1195** 1027–1030
[4] Kanel G I, Nellis W J, Savinykh A S, Razorenov S V and Rajendran A M 2009 *J. Appl. Phys.* **1195** 851
[5] Khishchenko K V 2015 *J. Phys.: Conf. Series* This issue (*Preprint* `arXiv:1510.00763`)
[6] Bushman A V, Lomonosov I V, Fortov V E and Khishchenko K V 1994 *Khim. Fizika* **13** 64–81
[7] Khishchenko K V 1997 *High Temp.* **35** 991–994
[8] Khishchenko K V, Lomonosov I V and Fortov V E 1998 *High Temp.–High Press.* **30** 373–378
[9] Wilkins M L 1963 *Calculation of Elastic-Plastic Flow* (Livermore, CA: Lawrence Radiation Laboratory, University of California)
[10] Liddiard Jr T P 1965 *Fourth Symposium on Detonation* p 214
[11] Barker L M and Hollenbach R E 1970 *J. Appl. Phys.* **41** 4208–4226
[12] Arzhakov M S, Lukovkin G M and Arzhakov S A 2002 *Chem. Phys. Rep.* **382** 1–4
[13] Kugotova A M and Kunizhev B I 2014 *Proc. Kabardino-Balkarian State University* **4** 44–47
[14] Genkin V N, Izvozchikova V A, Kitai M S and Mylnikov M Y 1985 *Quantum Electron.* **12** 2282
[15] Geras'kin A A, Khishchenko K V, Krasyuk I K, Pashinin P P, Semenov A Y and Vovchenko V I 2009 *Contrib. Plasma Phys.* **49** 451–454
[16] Abrosimov S A, Bazhulin A P, Voronov V V, Geras'kin A A, Krasyuk I K, Pashinin P P, Semenov A Y, Stuchebryukhov I A, Khishchenko K V and Fortov V E 2013 *Quantum Electron.* **43** 246–251
[17] Zel'dovich Y B and Raizer Y P 1967 *Physics of Shock Waves and High-Temperature Hydrodynamic Phenomena* (New York: Academic Press)
[18] McQueen R G and March D 1962 *J. Appl. Phys.* **33** 654–665
[19] Landau L D and Lifshitz E M 1987 *Fluid Mechanics* (Oxford: Elsevier)
[20] Landau L D and Lifshitz E M 1986 *Theory of Elasticity* (Oxford: Elsevier)
[21] Merzhievsky L A and Voronin M S 2012 *Proc. Altai State University* **1** 95–98
[22] Merzhievsky L A and Voronin M S 2012 *Combust. Expl. Shock Waves* **48** 226–235
[23] Birger I A and Mavlyutov R R 1986 *Resistance of Materials* (Moscow: Nauka)
[24] Lomonosov I V, Fortov V E and Khishchenko K V 1995 *Khim. Fizika* **14** 47–52
[25] Khishchenko K V, Lomonosov I V and Fortov V E 1996 *Shock Compression of Condensed Matter—1995* ed Schmidt S C and Tao W C (New York: AIP) pp 125–128
[26] Yalovets A P 1997 *J. Appl. Mech. Techn. Phys.* 51–66
[27] Kanel G I, Fortov V E and Razorenov S V 2007 *Phys. Usp.* **50** 771–791

[28] Farshad M, Wildenberg M W and Fliieler P 1997 *Mater. Struct.* **30** 377–382
[29] Bakanova A A, Dudoladov I P and Trunin R F 1965 *Sov. Phys. Solid State* **7** 1615–1622
[30] McQueen R G, Marsh S P, Taylor J W, Fritz J N and Carter W J 1970 *High Velocity Impact Phenomena* ed Kinslow R (New York: Academic Press) pp 293–417, 515–568
[31] Marsh S P 1980 *LASL Shock Hugoniot Data* (Berkeley, CA: Univ. California Press)
[32] Bushman A V, Zhernokletov M V, Lomonosov I V, Sutulov Y N, Fortov V E and Khishchenko K V 1993 *Dokl. Phys.* **38** 165–167
[33] Trunin R F 1994 *Phys. Usp.* **37** 1215–1237
[34] Maksanova L A 2004 *Polymer Compounds and Their Use* (Ulan-Ude: ESSTU Publishing)